Int. J. Solids Structures Vol. 30, No. 12, pp. 1701–1713, 1993
Printed in Great Britain

0020–7683/93 $6.00+ .00

A MODEL FOR MATRIX CRACKING IN SHORT FIBER COMPOSITES

GUNAY ANLAS and MICHAEL H. SANTARE
Department of Mechanical Engineering and Center for Composite Materials, University of Delaware, Newark, DE 19716, U.S.A.

(*Received* 12 *November* 1991; *in revised form* 4 *November* 1992)

Abstract—To model the crack–fiber interaction in the case of matrix cracking in short fiber composites, the plane problem of an elastic elliptical inclusion interacting with an arbitrarily oriented crack is solved, where the fiber is modeled as an elliptical inclusion. Complex potentials presented by Stagni and Lizzio (1983, *J. Appl. Phys.* **A30,** 217–221) are used to obtain the Green's function for this problem. The problem is formulated in terms of systems of singular integral equations which are solved numerically. Some detailed results are given for various crack and fiber geometries and fiber and matrix material combinations.

1. INTRODUCTION

To increase the application of short fiber reinforced composites, their behavior under different loading conditions should be understood. For example, matrix cracks may develop under monotonic and cyclic loadings in the case of weak fiber–matrix interface. This will result in a change in stiffness and strength of the material. Also, the understanding of the interaction of the already existing crack with the fiber is very important because one possible mechanism of toughening is the deflection of the crack by the existence of the fiber. Crack growth in short fiber composites can be studied by applying the following crack–inclusion interaction model where the effect of the presence of the inclusion can be seen in the change in stress intensity factors.

There have been a number of studies to understand the effect of inclusions on fracture. In previous work, specific studies on crack inclusion problems, such as circular inclusion–crack interaction or rigid elliptical inclusion–crack interaction problems, have been conducted. This study is more general since it allows for general elastic elliptical inclusions ranging in stiffness from a hole to a rigid inclusion. Atkinson (1972) used the solution of the edge dislocation–circular inclusion interaction problem presented by Dundurs and Mura (1964) to analyse the interaction between a crack with a circular inclusion. He set up the problem in terms of the distribution of dislocations and solved the resulting integral equations. Erdogan *et al.* (1974) studied the interaction between a circular inclusion and an arbitrarily oriented crack. They used a method similar to that of Atkinson's. Erdogan and Gupta (1975) later solved the case where the crack crosses the interface.

Elliptical inclusions were considered later than circular inclusions. Warren (1983) used an infinite series to formulate the problem where the edge dislocation is inside the elliptic inclusion. He later used the solution to study the stress field around a crack at the tip of a craze (Warren, 1984). Xue-Hui and Erdogan (1986) studied the interaction of a crack with a flat inclusion using the potentials given by Dundurs (1969) as Green's functions. Santare and Keer (1986) presented the solution for the interaction of an edge dislocation outside of a rigid elliptical inclusion. Using that solution to formulate the Green's functions, Patton and Santare (1990) studied the effect of a rigid elliptical inclusion on a straight crack. They later used this solution to study crack deflection near rigid inclusions and holes (1992). Wu and Chen (1990) solved the case where the crack was inside an elastic ellipse, where the crack extends from focus to focus of the ellipse. Luo and Chen (1991) modeled the matrix

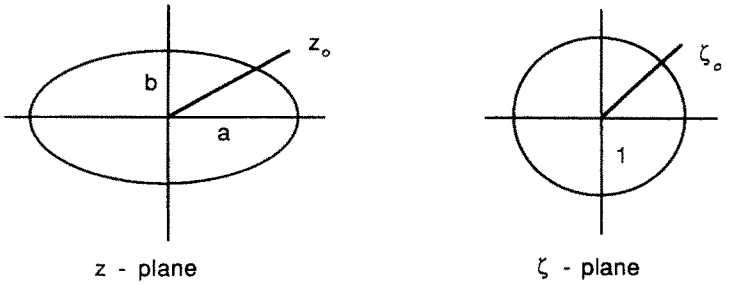

Fig. 1. Geometry of the problem: (a) physical; (b) mapped plane.

cracking by using a three phase cylindrical model. In an earlier paper, Anlas and Santare (1992) presented the solution for the case where an arbitrarily oriented crack is located inside an elliptical inclusion. This solution is later used to model fiber cracking in short fiber composites.

In this paper, the solution for an arbitrarily oriented crack interacting with an elastic elliptical inclusion is given. It is assumed that the elastic matrix contains short fibers that are distributed in such a way that there is no mechanical interaction between any two fibers. The only interaction is between the crack and the short fiber which is modeled as an elliptical inclusion. The crack is formulated in terms of a distribution of dislocations. Resulting integral equations are solved for the dislocation distribution which is used to calculate stress intensity factors.

2. THE STRESS FIELD FOR THE INTERACTION BETWEEN AN EDGE DISLOCATION AND ELLIPTICAL INCLUSION

Consider an elastic matrix, denoted as region 1, with elastic constants μ_1 and κ_1 containing a perfectly bonded elliptical elastic inclusion, denoted as region 2, with elastic consants κ_2 and μ_2, where μ_i is the shear modulus and $\kappa_i = 3-4\nu_i$ for plane strain and $\kappa_i = (3-\nu_i)/(1+\nu_i)$ for plane stress, and ν_i is the Poisson's ratio. The matrix contains an edge dislocation at point z_0 (see Fig. 1).

Stresses and displacements can be written in terms of the complex potentials as defined by Muskhelishvili (1953):

$$\sigma_{xx}+\sigma_{yy} = 2[\phi'(z)+\overline{\phi'(z)}], \tag{1}$$

$$\sigma_{yy}-\sigma_{xx}+2i\sigma_{xy} = 2[\bar{z}\phi''(z)+\psi'(z)], \tag{2}$$

$$2\mu(u+iv) = \kappa\phi(z)-z\overline{\phi'(z)}-\overline{\psi'(z)}. \tag{3}$$

The primes denote the derivatives with respect to z, where $z = x+iy$, the overbar denotes the complex conjugate and i is the imaginary number. The stress field in the matrix with the dislocation has been solved in terms of the complex potentials ϕ and ψ presented by Stagni and Lizzio (1983).

The geometry of the problem is simplified by mapping the ellipse into the unit circle as shown on Fig. 1, the function used is

$$z = w(\zeta) = R\left(\zeta+\frac{m}{\zeta}\right), \quad \text{where} \quad m = \frac{a-b}{a+b} \quad \text{and} \quad R = \frac{a+b}{2}.$$

The complex potentials ϕ_1 and ψ_1 for region 1 are

$$\phi_1(\zeta) = \gamma_1 \ln\left[\frac{(\zeta-\zeta_0)\left(\zeta-\dfrac{m}{\zeta_0}\right)}{\zeta}\right] + \sum_{-\infty}^{\infty} c_k \zeta^k, \tag{4}$$

$$\psi_1(\zeta) = \bar{\gamma}_1 \ln\left[\frac{(\zeta-\zeta_0)\left(\zeta-\dfrac{m}{\zeta_0}\right)}{\zeta}\right] + \gamma_1 \frac{\zeta\left(\dfrac{1}{\zeta}+m\zeta-\bar{\zeta}_0-\dfrac{m}{\bar{\zeta}_0}\right)}{(\zeta-\zeta_0)(\zeta-m/\zeta_0)} + \sum_{-\infty}^{\infty} d_k \zeta^k$$

$$-\gamma_1 \frac{\zeta(1+m\zeta^2)}{\zeta^2-m} \frac{\zeta_0\zeta^2-m\zeta_0}{\zeta_0\zeta^3-(m+\zeta_0^2)\zeta^2+\zeta_0 m\zeta} - \frac{\zeta(1+m\zeta^2)}{\zeta^2-m} \sum_{-\infty}^{\infty} c_k k \zeta^{(k-1)}. \tag{5}$$

In these expressions, $\gamma_1 = \mu_1 \mathbf{b}/i\pi(\kappa_1+1)$, where $\mathbf{b} = b_x + ib_y$, and b_x and b_y are the Cartesian components of the Burger's vector. The constants c_k and d_k in the series are defined in the Appendix.

Therefore, after some manipulations, we can write the stresses in region 1 as:

$$\sigma_{xx} = \gamma_1 \frac{\zeta\zeta_0}{R(\zeta-\zeta_0)(\zeta\zeta_0-m)} + \frac{\zeta^2}{R(\zeta^2-m)} \sum_{-\infty}^{\infty} c_k k \zeta^{k-1}$$

$$+\text{Conj}\left[\gamma_1 \frac{\zeta\zeta_0}{R(\zeta-\zeta_0)(\zeta\zeta_0-m)} + \frac{\zeta^2}{R(\zeta^2-m)} \sum_{-\infty}^{\infty} c_k k \zeta^{k-1}\right]$$

$$+\text{Re}\left[\gamma_1 \frac{(m+\bar{\zeta}^2)\zeta_0^2\zeta^2}{\bar{\zeta} R(\zeta-\zeta_0)^2(\zeta_0\zeta-m)^2} + \frac{2m\zeta^3(\bar{\zeta}^2+m)}{R\bar{\zeta}(\zeta^2-m)^3} \sum_{-\infty}^{\infty} c_k k \zeta^{k-1}\right.$$

$$-\frac{(\bar{\zeta}^2+m)\zeta^4}{R(\zeta^2-m)^2\bar{\zeta}} \sum_{-\infty}^{\infty} c_k k(k-1)\zeta^{k-2} - \bar{\gamma}_1 \frac{\zeta\zeta_0}{R(\zeta-\zeta_0)(\zeta\zeta_0-m)}$$

$$-\gamma_1 \frac{(m+\bar{\zeta}_0^2)\zeta_0^2\zeta^2}{\bar{\zeta}_0 R(\zeta-\zeta_0)^2(\zeta_0\zeta-m)^2} - \frac{\zeta^2}{R(\zeta^2-m)} \sum_{-\infty}^{\infty} d_k k \zeta^{k-1}$$

$$\left.+\frac{\zeta^2(m\zeta^4-3m^2\zeta^2-\zeta^2-m)}{R(\zeta^2-m)^3} \sum_{-\infty}^{\infty} c_k k \zeta^{k-1} + \frac{\zeta^3(1+m\zeta^2)}{R(\zeta^2-m)^2} \sum_{-\infty}^{\infty} c_k k(k-1)\zeta^{k-2}\right], \tag{6}$$

$$\sigma_{yy} = \gamma_1 \frac{\zeta\zeta_0}{R(\zeta-\zeta_0)(\zeta\zeta_0-m)} + \frac{\zeta^2}{R(\zeta^2-m)} \sum_{-\infty}^{\infty} c_k k \zeta^{k-1}$$

$$+\text{Conj}\left[\gamma_1 \frac{\zeta\zeta_0}{R(\zeta-\zeta_0)(\zeta\zeta_0-m)} + \frac{\zeta^2}{R(\zeta^2-m)} \sum_{-\infty}^{\infty} c_k k \zeta^{k-1}\right]$$

$$-\text{Re}\left[\gamma_1 \frac{(m+\bar{\zeta}^2)\zeta_0^2\zeta^2}{\bar{\zeta} R(\zeta-\zeta_0)^2(\zeta_0\zeta-m)^2} + \frac{2m\zeta^3(\bar{\zeta}^2+m)}{R\bar{\zeta}(\zeta^2-m)^3} \sum_{-\infty}^{\infty} c_k k \zeta^{k-1}\right.$$

$$-\frac{(\bar{\zeta}^2+m)\zeta^4}{R(\zeta^2-m)^2\bar{\zeta}} \sum_{-\infty}^{\infty} c_k k(k-1)\zeta^{k-2} - \bar{\gamma}_1 \frac{\zeta\zeta_0}{R(\zeta-\zeta_0)(\zeta\zeta_0-m)}$$

$$-\gamma_1 \frac{(m+\bar{\zeta}_0^2)\zeta_0^2\zeta^2}{\bar{\zeta}_0 R(\zeta-\zeta_0)^2(\zeta_0\zeta-m)^2} - \frac{\zeta^2}{R(\zeta^2-m)} \sum_{-\infty}^{\infty} d_k k \zeta^{k-1}$$

$$\left.+\frac{\zeta^2(m\zeta^4-3m^2\zeta^2-\zeta^2-m)}{R(\zeta^2-m)^3} \sum_{-\infty}^{\infty} c_k k \zeta^{k-1} + \frac{\zeta^3(1+m\zeta^2)}{R(\zeta^2-m)^2} \sum_{-\infty}^{\infty} c_k k(k-1)\zeta^{k-2}\right], \tag{7}$$

$$\sigma_{xy} = \mathrm{Im}\left[-\gamma_1 \frac{(m+\bar{\zeta}^2)\zeta_0^2\zeta^2}{\bar{\zeta}R(\zeta-\zeta_0)^2(\zeta_0\zeta-m)^2} - \frac{2m\zeta^3(\bar{\zeta}^2+m)}{R\bar{\zeta}(\zeta^2-m)^3} \sum_{-\infty}^{\infty} c_k k\zeta^{k-1} \right.$$

$$+ \frac{(\bar{\zeta}^2+m)\zeta^4}{R(\zeta^2-m)^2\bar{\zeta}} \sum_{-\infty}^{\infty} c_k k(k-1)\zeta^{k-2} + \bar{\gamma}_1 \frac{\zeta\zeta_0}{R(\zeta-\zeta_0)(\zeta\zeta_0-m)}$$

$$+ \gamma_1 \frac{(m+\bar{\zeta}_0^2)\zeta_0^2\zeta^2}{\bar{\zeta}_0 R(\zeta-\zeta_0)^2(\zeta_0\zeta-m)^2} + \frac{\zeta^2}{R(\zeta^2-m)} \sum_{-\infty}^{\infty} d_k k\zeta^{k-1}$$

$$\left. - \frac{\zeta^2(m\zeta^4-3m^2\zeta^2-\zeta^2-m)}{R(\zeta^2-m)^3} \sum_{-\infty}^{\infty} c_k k\zeta^{k-1} - \frac{\zeta^3(1+m\zeta^2)}{R(\zeta^2-m)^2} \sum_{-\infty}^{\infty} c_k k(k-1)\zeta^{k-2} \right]. \quad (8)$$

These stresses can be separated into bounded and singular portions. The singular portions representing the dislocation and its image points, the bounded portion representing the interaction for the case where the crack is fully imbedded in the matrix without touching the interface. The bounded parts of the stresses are calculated by matching the tractions and displacements along the elliptical contour which is mapped to the unit circle. The resulting terms are the series terms of the expressions above:

$$\sigma_{xxb} = 2\frac{\zeta^2}{R(\zeta^2-m)} \sum_{-\infty}^{\infty} c_k k\zeta^{k-1} + \mathrm{Re}\left[\frac{2m\zeta^3(\bar{\zeta}^2+m)}{R\bar{\zeta}(\zeta^2-m)^3} \sum_{-\infty}^{\infty} c_k k\zeta^{k-1} \right.$$

$$- \frac{(\bar{\zeta}^2+m)\zeta^4}{R(\zeta^2-m)^2\bar{\zeta}} \sum_{-\infty}^{\infty} c_k k(k-1)\zeta^{k-2} - \frac{\zeta^2}{R(\zeta^2-m)} \sum_{-\infty}^{\infty} d_k k\zeta^{k-1}$$

$$\left. + \frac{\zeta^2(m\zeta^4-3m^2\zeta^2-\zeta^2-m)}{R(\zeta^2-m)^3} \sum_{-\infty}^{\infty} c_k k\zeta^{k-1} + \frac{\zeta^3(1+m\zeta^2)}{R(\zeta^2-m)^2} \sum_{-\infty}^{\infty} c_k k(k-1)\zeta^{k-2} \right]. \quad (9)$$

$$\sigma_{yyb} = 2\frac{\zeta^2}{R(\zeta^2-m)} \sum_{-\infty}^{\infty} c_k k\zeta^{k-1} + \mathrm{Re}\left[\frac{2m\zeta^3(\bar{\zeta}^2+m)}{R\bar{\zeta}(\zeta^2-m)^3} \sum_{-\infty}^{\infty} c_k k\zeta^{k-1} \right.$$

$$- \frac{(\bar{\zeta}^2+m)\zeta^4}{R(\zeta^2-m)^2\bar{\zeta}} \sum_{-\infty}^{\infty} c_k k(k-1)\zeta^{k-2} - \frac{\zeta^2}{R(\zeta^2-m)} \sum_{-\infty}^{\infty} d_k k\zeta^{k-1}$$

$$\left. + \frac{\zeta^2(m\zeta^4-3m^2\zeta^2-\zeta^2-m)}{R(\zeta^2-m)^3} \sum_{-\infty}^{\infty} c_k k\zeta^{k-1} + \frac{\zeta^3(1+m\zeta^2)}{R(\zeta^2-m)^2} \sum_{-\infty}^{\infty} c_k k(k-1)\zeta^{k-2} \right]. \quad (10)$$

$$\sigma_{xyb} = \mathrm{Im}\left[\frac{2m\zeta^3(\bar{\zeta}^2+m)}{R\bar{\zeta}(\zeta^2-m)^3} \sum_{-\infty}^{\infty} c_k k\zeta^{k-1} \right.$$

$$- \frac{(\bar{\zeta}^2+m)\zeta^4}{R(\zeta^2-m)^2\bar{\zeta}} \sum_{-\infty}^{\infty} c_k k(k-1)\zeta^{k-2} - \frac{\zeta^2}{R(\zeta^2-m)} \sum_{-\infty}^{\infty} d_k k\zeta^{k-1}$$

$$\left. + \frac{\zeta^2(m\zeta^4-3m^2\zeta^2-\zeta^2-m)}{R(\zeta^2-m)^3} \sum_{-\infty}^{\infty} c_k k\zeta^{k-1} + \frac{\zeta^3(1+m\zeta^2)}{R(\zeta^2-m)^2} \sum_{-\infty}^{\infty} c_k k(k-1)\zeta^{k-2} \right]. \quad (11)$$

The singular portions of the stresses are the remaining terms which are not represented in the above series.

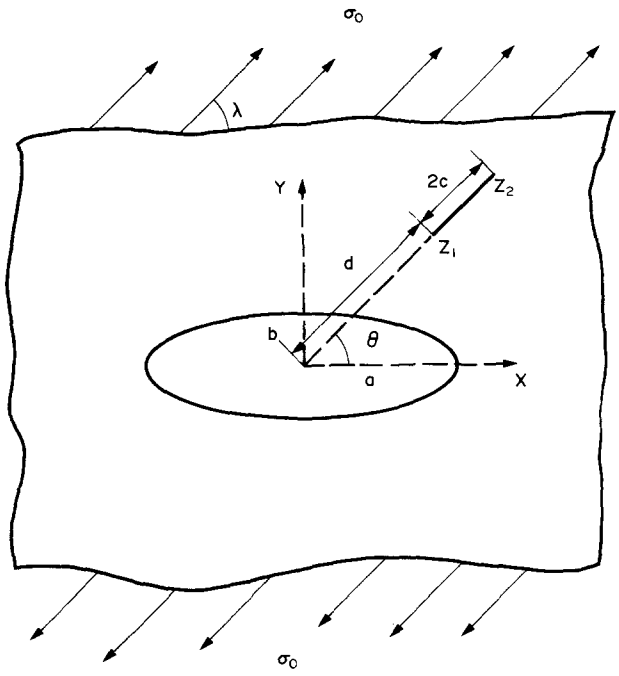

Fig. 2. Problem geometry.

3. INTEGRAL EQUATIONS

A crack can be represented by a distribution of dislocations. In this case the distribution is unknown, but the resulting crack faces are assumed to be traction free. This condition can be expressed by the following integral equations:

$$\int_{z_1}^{z_2} \frac{b_n(z_0)}{z-z_0}\,dz_0 + \int_{z_1}^{z_2} K_n(z,z_0)b_n(z_0)\,dz_0 = \frac{\pi(\kappa_1+1)}{\mu_1}F_n(z), \tag{12}$$

$$\int_{z_1}^{z_2} \frac{b_t(z_0)}{z-z_0}\,dz_0 + \int_{z_1}^{z_2} K_t(z,z_0)b_t(z_0)\,dz_0 = \frac{\pi(\kappa_1+1)}{\mu_1}F_t(z). \tag{13}$$

n and t refer to the positive normal and tangential directions to the crack. b_n and b_t are defined as:

$$b_n = b_y\cos\theta - b_x\sin\theta, \tag{14}$$

$$b_t = b_y\sin\theta + b_x\cos\theta, \tag{15}$$

where θ is the angle of the crack as shown in Fig. 2.

The first integrals contain the Cauchy singular portion of the stresses due to distribution of dislocations. K_n and K_t, in the second integrals, are the bounded kernels which represent the interaction between the crack and the elliptic inclusion. They are in the n and t directions respectively. Some portions of K_n and K_t become unbounded when the crack touches the interface between the inclusion and the matrix. This situation requires a separate analysis as discussed in Erdogan and Gupta (1975) and is not treated here. K_n and K_t can be obtained from eqns (9)–(11):

$$K_n b_n = \sigma_{xxb}\cos^2\theta + \sigma_{yyb}\sin^2\theta + 2\sigma_{xyb}\sin\theta\cos\theta, \tag{16}$$

$$K_t b_t = (\sigma_{yyb}-\sigma_{xxb})\sin\theta\cos\theta + \sigma_{xyb}(\cos^2\theta-\sin^2\theta). \tag{17}$$

b_n and b_t are also contained in σ_{xxb}, σ_{yyb} and σ_{xyb}. The terms on the right-hand side of the

integral equations [eqns (12) and (13)], are the stresses in region 1, due to far field loading and in the absence of the dislocations.

4. THE PROBLEM OF AN ELASTIC ELLIPTICAL INCLUSION IN A MATRIX WITHOUT A CRACK

To solve the crack–ellpitical inclusion interaction problem, the solution of the problem of an elliptical inclusion inserted in an infinite matrix is needed. This solution becomes the right-hand side of eqns (12) and (13). The system will be subject to stress σ_0 at infinity as shown in Fig. 2. The solution can be obtained by following the method given by Muskhelishvili (1953) [see also Qaissaunee (1992)]. The complex potentials for region 1 are

$$\phi_1^0(\zeta) = a_{-1}\zeta + a_1\zeta, \tag{18}$$

$$\eta_1^0(\zeta) = b_{-1}\zeta + b_1\zeta. \tag{19}$$

$a_1 = R\sigma_0/4$ and $b_1 = R\sigma_0/2(m/2 - e^{2i\alpha})$. a_{-1} and b_{-1} are found using the traction and displacement continuity along the elliptical boundary between regions 1 and 2, the inclusion and the matrix, in the absence of a crack:

$$b_{-1} = \frac{1}{\beta}(\alpha\bar{c}_1 + md_1 + q_1c_1), \tag{20}$$

$$a_{-1} = \frac{1}{\beta}[(\beta-\alpha)c_1 + (\beta-1)\bar{d}_1], \tag{21}$$

where

$$c_1 = \frac{\beta(p_1r_1 - (\beta-1)q_1\bar{r}_1)}{p_1^2 - (\beta-1)^2q_1^2}, \tag{22}$$

$$d_1 = \beta b_1 - \alpha m\bar{c}_1, \tag{23}$$

$$q_1 = 1 - m^2, \tag{24}$$

$$p_1 = (\beta-\alpha) - (\beta-1)\alpha m^2, \tag{25}$$

$$\alpha = \frac{\Gamma\kappa_1 - \kappa_2}{\Gamma\kappa_1 + 1}, \tag{26}$$

$$\beta = \frac{\Gamma(\kappa_1 + 1)}{\Gamma\kappa_1 + 1}, \tag{27}$$

and σ_0 is the stress at infinity.

By using the potentials given in eqns (18) and (19) and eqns (20)–(27) the stresses outside the inclusion, the right-hand sides of the integral equations, are found.

5. SOLUTION

The integral equations can be reduced to a standard form by the substitutions

$$z_0 = \frac{z_2 - z_1}{2}\xi_0 + \frac{z_2 + z_1}{2}, \tag{28}$$

$$z = \frac{z_2 - z_1}{2}\xi + \frac{z_2 + z_1}{2}. \tag{29}$$

Equations (25) and (26) can now be written in the form:

$$\int_{-1}^{1} \frac{b_n(\xi_0)}{c(\xi - \xi_0)}\,d\xi_0 + \int_{-1}^{1} K_n(\xi, \xi_0) b_n(\xi_0)\,d\xi_0 = \frac{\pi(\kappa_1 + 1)}{\mu_1} F_n(\xi), \tag{30}$$

$$\int_{-1}^{1} \frac{b_t(\xi_0)}{c(\xi - \xi_0)}\,d\xi_0 + \int_{-1}^{1} K_t(\xi, \xi_0) b_t(\xi_0)\,d\xi_0 = \frac{\pi(\kappa_1 + 1)}{\mu_1} F_t(\xi), \tag{31}$$

where $c = (z_2 - z_1)/2$.

To find a unique solution to the integral equations, it is necessary to impose an additional condition such as the crack closure condition:

$$\int_{-1}^{1} b_n(\xi_0)\,d\xi_0 = 0, \tag{32}$$

$$\int_{-1}^{1} b_t(\xi_0)\,d\xi_0 = 0. \tag{33}$$

The unknown functions can be defined as follows:

$$b_n(\xi_0) = \frac{g_n(\xi_0)}{\sqrt{1 - \xi_0^2}}, \tag{34}$$

$$b_t(\xi_0) = \frac{g_t(\xi_0)}{\sqrt{1 - \xi_0^2}}, \tag{35}$$

which gives the square root singularity for a crack tip surrounded by a homogeneous medium. The system of singular integral equations is solved by the method described by Gerasoulis (1982). The interval $[-1, 1]$ is divided into $2n$ equal parts with $2n$ collocation points and $2n+1$ integration points. Piecewise quadratic polynomial representation of the singular and non-singular parts of the integral equation is used to discretize the integral equations into a set of algebraic equations. The strengths of the stress singularity at the crack tips are characterized by the stress intensity factors. They are related to the dislocation density functions as follows:

$$K_I(z_1) = \frac{2\mu_1}{1 + \kappa_1} \lim_{z \to z_1} [2(z_1 - z)]^{1/2} b_n(z), \tag{36}$$

$$K_I(z_2) = \frac{2\mu_1}{1 + \kappa_1} \lim_{z \to z_2} [2(z - z_2)]^{1/2} b_n(z), \tag{37}$$

$$K_{II}(z_1) = \frac{2\mu_1}{1 + \kappa_1} \lim_{z \to z_1} [2(z_1 - z)]^{1/2} b_t(z), \tag{38}$$

Table 1. Stress intensity factors for a crack interacting with a circular inclusion, $m = 0.0$, $\theta = 0.0°$, $\kappa_1 = 1.6$, $\kappa_2 = 1.8$, $\lambda = 90.0°$, $2a = x_2 - x_1$, $2b = x_2 + x_1$, $c/R = 1.0$ comparison of results of Erdogan and Gupta (E&G) and Anlas and Santare (A&S)

	$\mu_2 = 0.0$		$\mu_2/\mu_1 = 23$	
b/a	E&G	A&S	E&G	A&S
3.2	2.274	2.276	0.827	0.834
3.5	1.722	1.721	0.874	0.881
4.0	1.394	1.394	0.918	0.925
5.0	1.174	1.174	0.957	0.962
6.0	1.099	1.099	0.973	0.977
8.0	1.045	1.045	0.987	0.989

$$K_{II}(z_2) = \frac{2\mu_1}{1+\kappa_1} \lim_{z \to z_2} [2(z-z_2)]^{1/2} b_1(z). \tag{39}$$

K_I and K_{II} are mode I and mode II stress intensity factors, respectively.

6. RESULTS

This analysis can be used to predict crack propagation in short fiber reinforced composites. The effect of the fiber on the crack can be measured by evaluating the stress intensity factors for different crack fiber geometries. Numerical results are given for the stress intensity factors defined by (36)–(39). Stress intensity factors for cracks interacting with elliptical inclusions of different ellipticity m can be solved by changing the parameters in the solution outlined above. The problem can also be solved for stresses applied at different angles at infinity. In the following, crack–fiber interactions are studied extensively for various crack angles and various fiber aspect ratios. The results of $m = 0$, crack interacting with a circular inclusion, with uniaxial stresses applied at infinity are compared to the results presented by Erdogan and Gupta (1975) and are shown in Table 1. The stress intensity factors are normalized with respect to $\sigma_0/\sqrt{c}$ which is the stress intensity factor in a uniaxially stressed infinite plane containing a crack of length $2c$ perpendicular to the direction of loading.

In Fig. 3, mode I stress intensity factors are given for a straight crack. Results for different distances from the inclusion are plotted for $\mu_2/\mu_1 \to \infty$, rigid inclusion and elastic matrix (for example, for Boron–Epoxy, $\mu_2/\mu_1 = 138$), for inclusions having different aspect ratios. The normalized stress intensity factors converge to 1.0 when the crack is sufficiently far away from the inclusion. It is seen that vertically oriented elliptical inclusions, $m < 0.0$, decrease the stress intensity factors more than the ones that are oriented horizontally, $m > 0.0$.

In Fig. 4, a straight crack interacting with elastic elliptical inclusion is shown. To show the effect of the rigidity on the stress intensity factors, the results are plotted for different values of shear modulus ratios. Several aspect ratios are plotted. It is shown that the rigidity of the inclusion is a big factor in the change of stress intensity factors especially for vertically oriented ellipses. Beyond a μ_2/μ_1 value of 25 the stress intensity factors stop being affected greatly, and converge. In other words, after a certain rigidity ratio, the results approach the results of a rigid inclusion.

SIFs for a circular inclusion, $m = 0.0$, are given in Fig. 5. In this case the effect of crack inclination on the stress intensity factor is studied. The ratio of shear moduli, μ_2/μ_1, is 23.08 which is the case of epoxy–aluminum. When the crack crosses over to 50° and above the stress intensity factors decrease instead of increasing as expected.

Similar results are given in Fig. 6 for a rigid elliptical inclusion. In this case the crack is at a distance of 0.1 from the interface for each case. But the results are plotted for different crack angles and for elliptical inclusions with different aspect ratios. The effect of the crack angle is very big when the crack is close to the interface. For increased values of crack angles the stress intensity factors almost converge to the same value even for different m

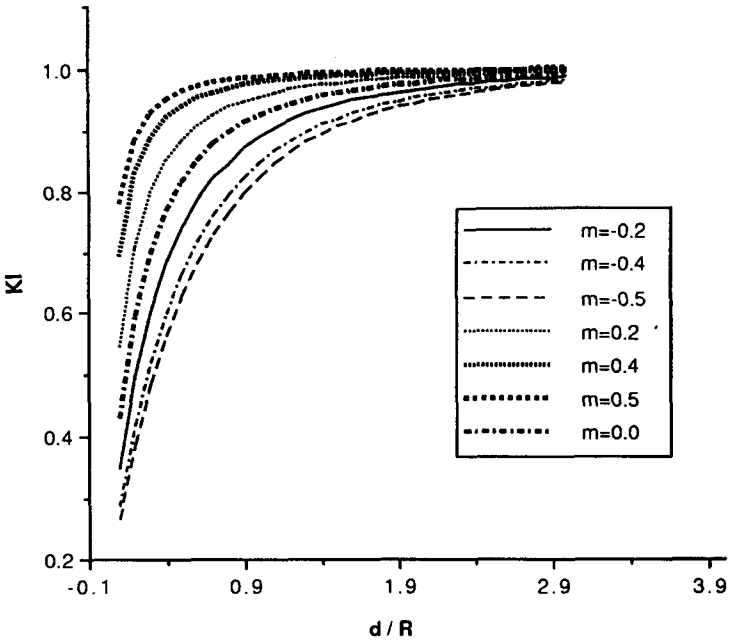

Fig. 3. Normalized stress intensity factor vs distance from interface, for different values of m, $\lambda = 90.0°$, $2c/R = 1.0$, $\mu_2/\mu_1 \to \infty$, $\kappa_1 = 1.6$, $\theta = 0.0$ (Epoxy–Boron).

values. The fact that the SIFs are affected the most at small angles for flat inclusions, $m = 0.5$, $m = 0.7$, $m = 0.9$, can be explained by the shielding effect of the inclusion [see also Patton and Santare (1990)].

In Fig. 7, the case for a soft inclusion, $\mu_2/\mu_1 = 1/3$, is shown. To understand the effect of soft inclusions with varying ellipticity and to complete the information given by Fig. 7,

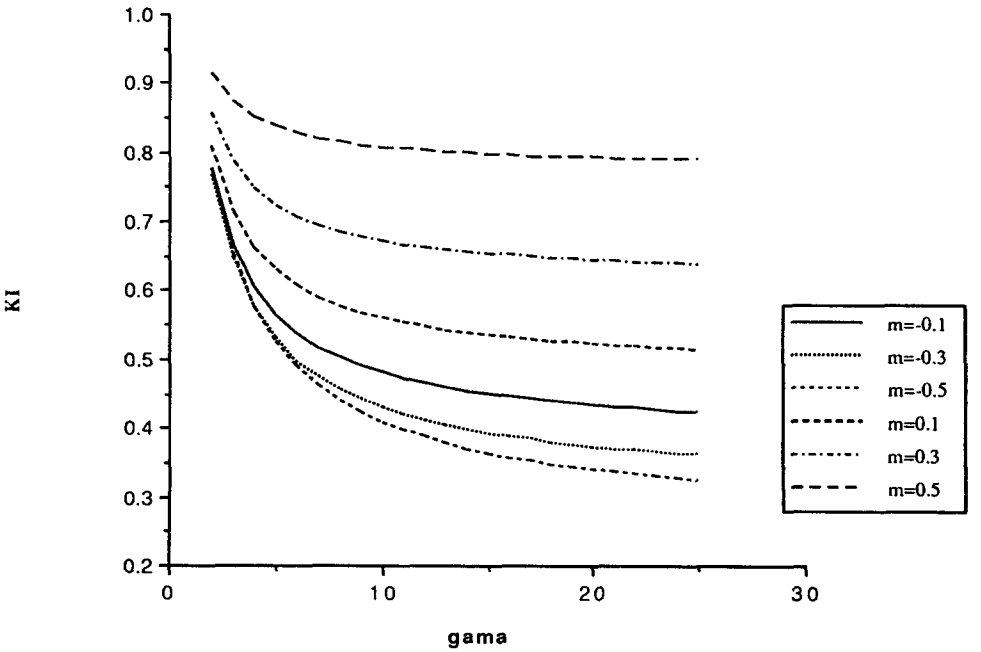

Fig. 4. Normalized stress intensity factor vs rigidity ratio $\gamma = \mu_2/\mu_1$, for different values of m, $\lambda = 90.0°$, $2c/R = 1.0$, $d/R = 0.1$, $\kappa_1 = 1.6$, $\kappa_2 = 1.8$, $\theta = 0.0$.

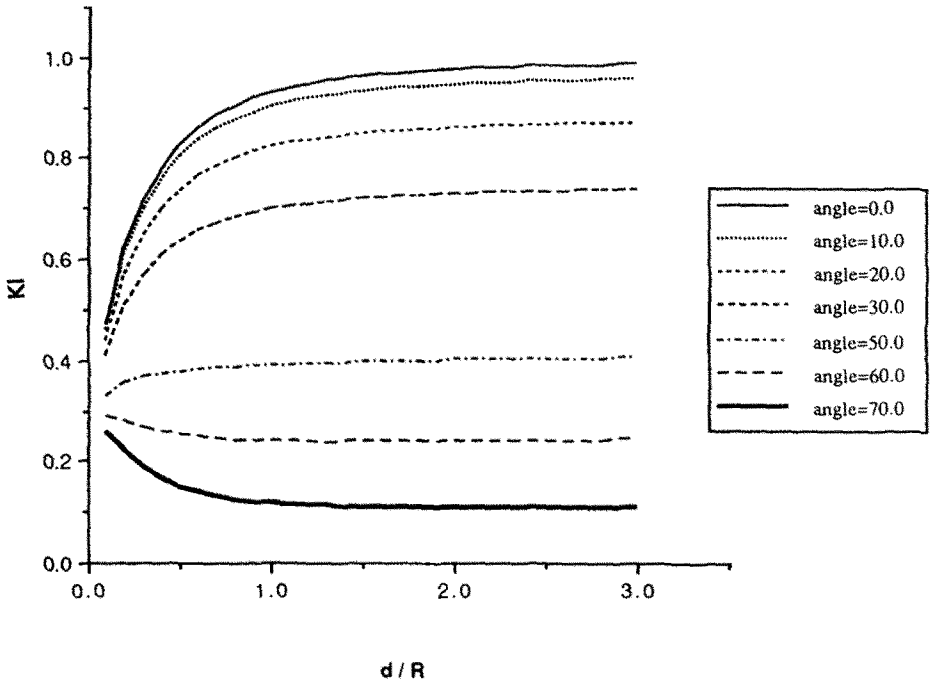

Fig. 5. Normalized stress intensity factor vs distance from interface, for different crack angles, θ, $m = 0.0$, $2c/R = 1.0$, $\mu_2/\mu_1 = 23.08$ (Epoxy–Al), $\kappa_1 = 1.6$, $\kappa_2 = 1.8$, $d/R = 0.1$.

Fig. 8 is presented. Figure 8 shows the shift in maximum stress intensity factor for different m values. This figure also explains the overlap that occurs with the introduction of $m = 0.0$ and $m = 0.2$ in Fig. 7. Maximum SIF occurs at $d/R = 0.1$ for a circular inclusion, but when the crack is further away, for instance when $d/R = 0.5$, the maximum SIF occurs at $m = -0.2$.

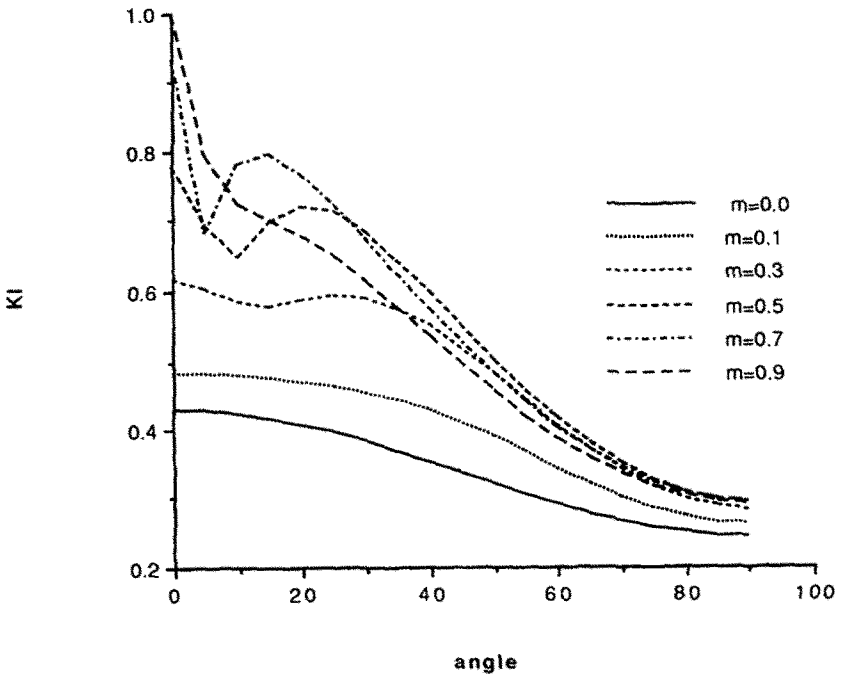

Fig. 6. Normalized stress intensity factor vs crack angle, θ, for different values of m, $\lambda = 90.0°$, $2c/R = 1.0$, $\mu_2/\mu_1 \to \infty$, $\kappa_1 = 1.6$, $d/R = 0.1$.

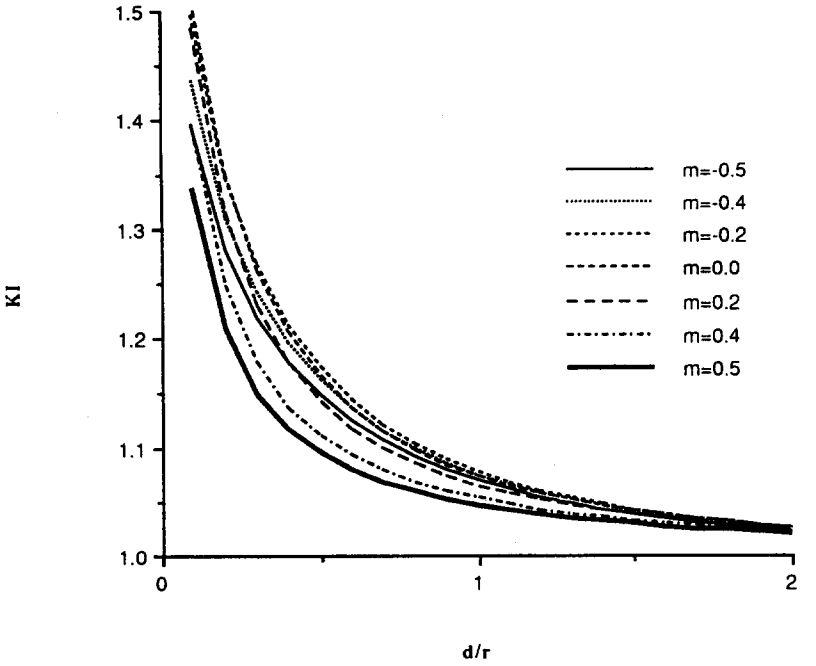

Fig. 7. Normalized stress intensity factor vs distance from interface, for different values of m, $\lambda = 90.0°$, $2c/R = 1.0$, $\mu_2/\mu_1 = 1/3$, $\kappa_1 = 1.6$, $\kappa_2 = 1.8$, $\theta = 0.0$ (Aluminum–Steel).

The stress intensity factors of a crack interacting with a rigid inclusion are compared with the experimental results given by O'Toole and Santare (1990) and they are in good agreement. In that study, they used photoelasticity to find the stress intensity factors for crack tips in polycarbonate (PSM-1) near steel inclusions. The stiffness ratio for the experimental system is about $\Gamma = 80$ which is a fair approximation to a rigid inclusion. In

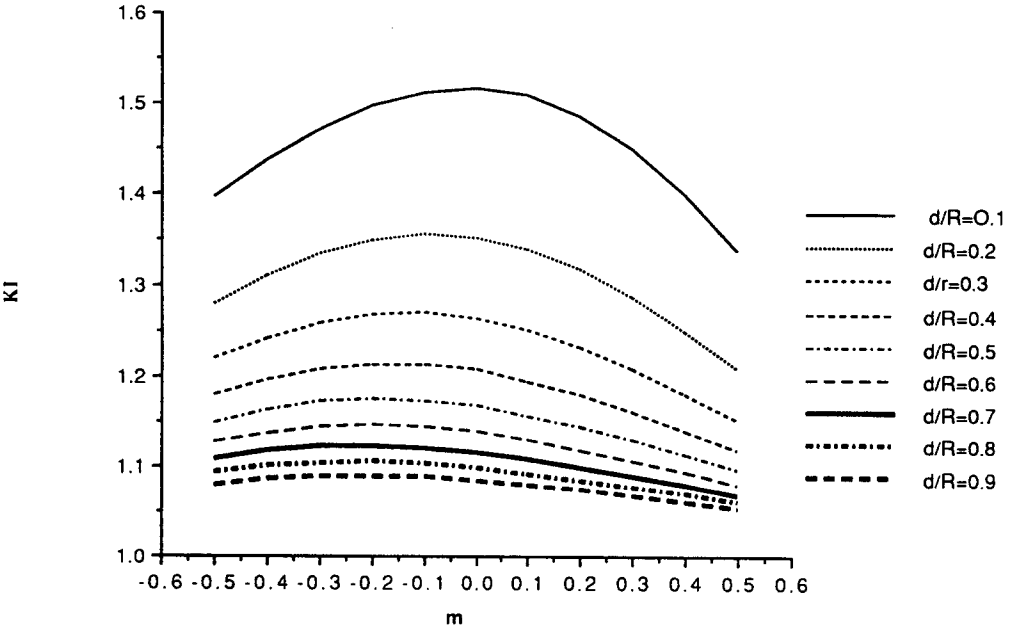

Fig. 8. Normalized stress intensity factor vs ellipticity m, for different values of d/R, $\lambda = 90.0°$, $2c/R = 1.0$, $\mu_2/\mu_1 = 1/3$, $\kappa_1 = 1.6$, $\kappa_2 = 1.8$, $\theta = 0.0$.

the majority of cases, the experimental and analytical results are within a few percent, but in some cases the difference can be as high as 19%. These differences can be due to experimental procedure as described in O'Toole and Santare (1990).

REFERENCES

Anlas, G. and Santare, M. H. (1992). Arbitrarily oriented crack inside an elliptical inclusion. *J. Appl. Mech.* (to appear).

Atkinson, C. (1972). The interaction between a crack and an inclusion. *Int. J. Engng Sci.* **10**, 127–136.

Dundurs, J. (1969). Elastic interaction of dislocations with inhomogeneities. In *Mathematical Theory of Dislocations* (Edited by T. Mura), pp. 70–115. ASME, New York.

Dundurs, J. and Mura, T. (1964). Interaction between an edge dislocation and a circular inclusion. *J. Mech. Phys. Solids* **12**, 177–189.

Erdogan, F. and Gupta, G. D. (1975). The inclusion problem with a crack crossing the boundary. *Int. J. Fracture* **11**(1), 13–27.

Erdogan, F., Gupta, G. D. and Ratwani, M. (1974). Interaction between a circular inclusion and an arbitrarily oriented crack. *J. Appl. Mech.* **41**, 1007–1013.

Gerasoulis, A. (1982). The use of piecewise quadratic polynomials for the solution of singular integral equations of Cauchy type. *Comput. Math. Appl.* **8**(1), 15–22.

Hardiman, N. J. (1954). Elliptic elastic inclusion in an infinite plate. *Q. J. Mech. Appl. Math.* **7**, 226–230.

Luo, H. A. and Chen, Y. (1991). Matrix cracking in fiber-reinforced composite materials. *J. Appl. Mech.* **58**, 846–848.

Muskhelishvili, N. I. (1953). *Some Basic Problems of Mathematical Theory of Elasticity* (3rd Edn). Noordhoff, Groningen.

O'Toole, B. J. and Santare, M. H. (1990). Photoelastic interaction of crack-inclusion interaction. *Expl Mech.* **30**(3), 253–257.

Patton, E. M. and Santare, M. H. (1990). The effect of rigid elliptical inclusion on a straight crack. *Int. J. Fracture* **46**, 71–79.

Patton, E. M. and Santare, M. H. (1992). The effect of path prediction near an elliptical inclusion. *Engng Fracture Mech.* (to appear).

Qaissaunee, M. (1992). Interaction between an edge dislocation and a single-phase and two-phase elliptical inclusion. M.S. Thesis, University of Delaware.

Santare, M. H. and Keer, L. M. (1986). Interaction between the edge dislocation and a rigid elliptical inclusion. *J. Appl. Mech.* **53**, 382–385.

Santare, M. H., O'Toole, B. J. and Patton, E. M. (1991). Two-dimensional crack inclusion effects. *J. Press. Ves. Technol.* **113**, 392–397.

Stagni, L. and Lizzio, R. (1983). Shape effects in the interaction between an edge dislocation and elliptic inclusion. *J. Appl. Phys.* **A30**, 217–221.

Warren, W. E. (1983). The edge dislocation inside an elliptical inclusion. *Mech. Mater.* **2**, 319–330.

Warren, W. E. (1984). Stress and displacement fields at the tip of craze containing a crack. *Polymer Engng Sci.* **24**(10), 814–819.

Wu, C. H. and Chen, C.-H. (1990). A crack in a confocal elliptic inhomogeneity embedded in an infinite medium. *J. Appl. Mech.* **57**, 91–96.

Xue-Hui, L. and Erdogan, F. (1986). The crack inclusion interaction problem. *Engng Fract. Mech.* **23**(5), 821–832.

APPENDIX

The constants that are used in the stress potentials are given by:

$$c_k = 0.0, \tag{A1}$$

$$d_k = 0.0, \tag{A2}$$

$$c_{-k} = \frac{(\beta-\alpha)}{\beta} a_{-k} + \frac{(\beta-1)}{\beta} \bar{b}_k - \gamma_1 A_{-k}, \tag{A3}$$

$$d_{-k} = \frac{\alpha}{\beta} \bar{a}_k + \frac{1}{\beta} b_{-k} - (\bar{\gamma}_1 A_k + \gamma_1 B_{-k}), \tag{A4}$$

where

$$a_k = \frac{\beta(p_k r_k - (\beta-1) q_k \bar{r}_k)}{p_k^2 - (\beta-1)^2 q_k^2}, \tag{A5}$$

$$b_k = \beta(\bar{\gamma}_1 A_k + \gamma_1 B_k) - \alpha m^k \bar{a}_k, \tag{A6}$$

$$a_{-k} = m^k a_k,$$

$$b_{-k} = m^k b_k + q_k a_k$$

$$r_k = \gamma_1 A_k - (\beta-1) m^k (\gamma_1 \bar{A}_k + \bar{\gamma}_1 \bar{B}_k), \tag{A7}$$

$$p_k = (\beta-\alpha)-(\beta-1)\alpha m^{2k}, \tag{A8}$$

$$q_k = (1-m^2)km^{(k-1)}, \tag{A9}$$

$$A_k = -\frac{1}{k}(\zeta_0)^{-k}, \tag{A10}$$

$$A_{-k} = m^k A_k, \tag{A11}$$

$$B_{-k} = \left[\frac{mq-m^3/\zeta_0-\zeta_0}{\zeta_0^2-m}\right]\left(\frac{m}{\zeta_0}\right)^{k-1}, \tag{A12}$$

$$B_k = -\left(\frac{m\zeta_0^3-q\zeta_0^2+\zeta_0}{\zeta_0^2-m}\right)\left(\frac{1}{\zeta_0}\right)^{k+1}, \tag{A13}$$

$$q = \zeta_0+m/\zeta_0,$$

$$\alpha = \frac{\Gamma\kappa_1-\kappa_2}{\Gamma\kappa_1+1},$$

$$\beta = \frac{\Gamma(\kappa_1+1)}{\Gamma\kappa_1+1}.$$